Original scientific paper

Informacije MIDEM
Journal of Microelectronics,
Electronic Components and Materials
Vol. 46, No. 3(2016), 142 – 148

Temperature and Injection Current dependent Electroluminescence for Evaluation of Single-Junction Single-Segment GaAs Laser Power Converter

Rok Kimovec[1], Henning Helmers[2], Andreas W. Bett[2] and Marko Topič[1]

[1]University of Ljubljana, Faculty of Electrical Engineering, Ljubljana, Slovenia
[2]Fraunhofer Institute for Solar Energy Systems ISE, Freiburg, Germany

Abstract: The spatial electroluminescence intensity and spectral measurements of photovoltaic devices under forward bias have proved to be fast and reliable characterization tools. They enable quick evaluation of material and manufacturing quality and provide information linked to local performance of photovoltaic devices in different operating conditions.

In this work, EL images of single-junction single-segment GaAs laser power converters (LPC) and their emission spectra depending on the injection current and LPC temperature are presented and analyzed. A shift of the EL emission peak to smaller energies and a decrease in EL intensity with increasing temperature are observed in spectrally resolved EL measurements. Negative temperature coefficients dEL/dT of EL intensity depending on the injection current are extracted from spatially resolved EL measurements. EL images of the LPCs under low and high injection currents are presented and evaluated.

Keywords: electroluminescence; laser power converter; Power-over-Fiber; power-by-light; spatial electroluminescence; spectral electroluminescence; LPC

Vpliv temperature in vzbujalnega toka na elektroluminiscenco enosegmentnih enospojnih pretvornikov laserske moči

Izvleček: Meritve prostorske in spektralne elektroluminiscence fotovoltaičnih struktur so se izkazale za zanesljivo in hitro karakterizacijsko orodje. Omogočajo nam vpogled v kvaliteto uporabljenega materiala in izdelave struktur ter nam podajo možnost vpogleda v spreminjanje kazalcev učinkovitosti pri spreminjajočih delovnih pogojih.

V tem delu so predstavljene meritve in analiza prostorske in spektralne elektroluminiscence v odvisnosti od delovne temperature in vzbujalnega toka za primer enosegmentnega enospojnega pretvornika laserske moči izdelanega iz GaAs. Z višanjem temperature se intenziteta izsevane svetlobe zmanjša, izsevani spekter pa se premakne proti nižjim energijam. Iz analize prostorske elektroluminiscence je izračunan negativni temperaturni koeficient intenzitete izsevane svetlobe dEL/dT pri različnih vzbujalnih tokovih. Predstavljena je analiza slik prostorske elektroluminiscence za primer majhnega in velikega vzbujalnega toka.

Ključne besede: elektroluminiscenca; pretvornik laserske moči; Moč-po-vlaknu; prostorska elektroluminiscenca; spektralna elektroluminiscenca

** Corresponding Author's e-mail: rok.kimovec@fe.uni-lj.si*

1 Introduction

Electroluminescence (EL) in photovoltaic (PV) devices is a phenomenon occurring due to radiative recombination of electrically excited charge carriers, resulting in the emission of photons from the PV device structure. The measurement of EL, coupled with theoretical knowledge, has become an important tool in assessing performance of PV devices in both scientific and indus-

trial environments [1–4], due to fast acquisition times of modern imaging devices.

For purposes of Power-over-Fiber (PoF) (or "power-by-light") [5, 6], where optical energy in the form of laser light is transferred through electrically nonconductive optical fiber, special types of PV devices (laser power converters (LPC)) are utilized to convert monochromatic light to electricity [7, 8]. As for all other PV devices, performance of LPCs is upwards limited [9] and it can be evaluated to some extent by the use of spatially and spectrally resolved EL measurements.

The aim of this work is to gain insight into spatially and spectrally resolved characterization techniques and performance of LPCs under various operation temperatures and current densities.

2 Motivation

PoF is an emerging technology used for powering various electronic devices in extreme environments, where benefits such as galvanic isolation and electromagnetic compatibility overcome the additional cost and complexity of such power supply systems [10, 11].

To gain in-depth understanding of PoF systems, evaluation of individual components has to be undertaken. In this work we concentrate on assessing the performance of LPCs using advanced spatially resolved characterization techniques. The LPC is the part of the system which is converting monochromatic light into electricity, thus providing electrical energy to an electronic device at a remote location. Since such systems are used for powering a variety of electronic devices (e.g. sensors [12], cameras [13], actuators, etc.) in many different environments (e.g. space [14], high magnetic fields [15], etc.), they must perform well in different operating conditions, such as variation in temperature and power requirements for different electronic devices.

In order to understand the behavior and performance of LPCs in different working conditions better, an analysis of EL at various temperatures and injection currents has been performed and is presented in this paper.

3 Description of specimen

The investigated LPC sample is a single-junction single-segment (SJ-SS) GaAs photovoltaic device fabricated at Fraunhofer ISE. The active region is a 3.65 µm thick *pin*-stack with an n-type emitter of 120 nm thickness. It employs 25 nm AlInP window-layer on top of the emitter which acts as a passivation layer (front surface field). The p-doped base layer follows a back surface field (BSF) layer in order to passivate the rear side of the active solar cell. A schematic representation of the device structure is shown in Figure 1 (a). The chip area is 3 mm x 3 mm square with front contact circular busbar design, which covers 2 mm^2 of the area. An image of the device under test (DUT) is shown in Figure 1 (b).

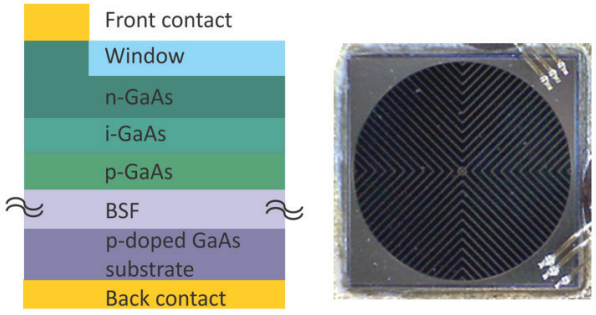

Figure 1: (a) Schematic of the investigated LPC. (b) Top view of 3 mm x 3 mm square LPC sample. Even though the device is wire bonded to a TO-header in two corners only the top right connection was used for measurement.

4 Experimental setup

In the following the experimental setup and procedures are described, that have been used to measure the spatially and spectrally resolved EL of SJ–SS GaAs LPC at the Laboratory of Photovoltaics and Optoelectronics at the Faculty of Electrical Engineering, University of Ljubljana. The results of the measurements of a SJ–SS GaAs LPC are presented and discussed.

4.1 General measurement description

To perform EL measurements, the LPC sample has been mounted on a temperature controlled chuck and placed into a light proof box, ensuring that only light irradiated by the LPC is measured.

Measurements of injection current and voltage were realized by four-wire connection at various injection current values, provided by an HP E363X series laboratory power supply operating in constant current mode. Current and voltage signals were measured with a pair of HP 34401A multimeters.

The measurement procedure for both spatial and spectral EL was as follows:

- Setting of desired injection current
- Setting of desired temperature

- Setting of acquisition time once the temperature was stable, to avoid saturation of the camera/spectrometer
- Measurement of spatial/spectral EL

4.2 Spatially resolved measurement setup

To obtain spatially resolved images a FLI MLx285 scientific camera was used, employing a Sony ICX285 CCD sensor (actively cooled to 0°C). The primary lens on the camera was a Schneider Optics NR56-534. Since the magnification with the primary lens was insufficient to take images of the small area LPC, a microscope objective was mounted on the primary lens with use of tube extenders and a custom made adapter. The described setup enables to acquire sharp EL images of small area LPCs with a resolution higher than 500x500 pixels.

4.3 Spectrally resolved measurement setup

EL spectra were measured with an Ocean Optics HR4000 spectrometer equipped with 600 µm core multimode optical fiber and cosine corrector. The setup was calibrated with a NIST traceable Ocean Optics LS-1-CAL light source prior to the EL measurements. The optical fiber input connector equipped with the cosine corrector was placed in close proximity above the LPC. At large injection currents the current distribution is expected to be non-uniform, leading to large differences of EL irradiation through the front surface of the LPC. Care was taken to assure that all irradiated light from the device under test was coupled into the fiber.

Even though the spectrum acquisition system was calibrated prior to measurement, it should be noted that such measurement systems are insufficient to measure absolute irradiance values, so that all spectral measurements results are expressed in arbitrary units. Still, they can serve for relative comparison of LPCs at varying operating conditions.

5 Results

5.1 Spatially resolved measurements

To perform analysis of images captured by the CCD camera, two corrections of the raw data were performed. First, the dark image was subtracted from all images. Second, individual pixel values were divided by acquisition time, resulting in each pixel value presented in counts per second acquired by the CCD. Further details on the measurement procedure and image manipulation procedure can be found elsewhere [16].

Acquired images from spatially resolved EL enable to perform two different types of analysis. First it is a qualitative analysis in which the material homogeneity can be evaluated at low injection currents. At high injection currents on the contrary, the influence of the busbar and sheet series resistances on the current distribution can be seen through the top layers of the device. The results of such an analysis are shown in Figure 2 and Figure 3 for two different injection currents (1 mA, 400 mA). Under the injection current of 1 mA (Figure 2) the LPC shows a mostly uniform electroluminescence across the whole cell area, which can be attributed to a homogeneous material quality of the GaAs crystal.

With an injection current of 400 mA (Figure 3), the measured EL intensity distribution across the LPC area decreases from the top right corner to the bottom left corner. This behavior can be explained by non-ideal contacting of the specimen. Opposed to an ideal contacting in each corner of the device, wire bonds were

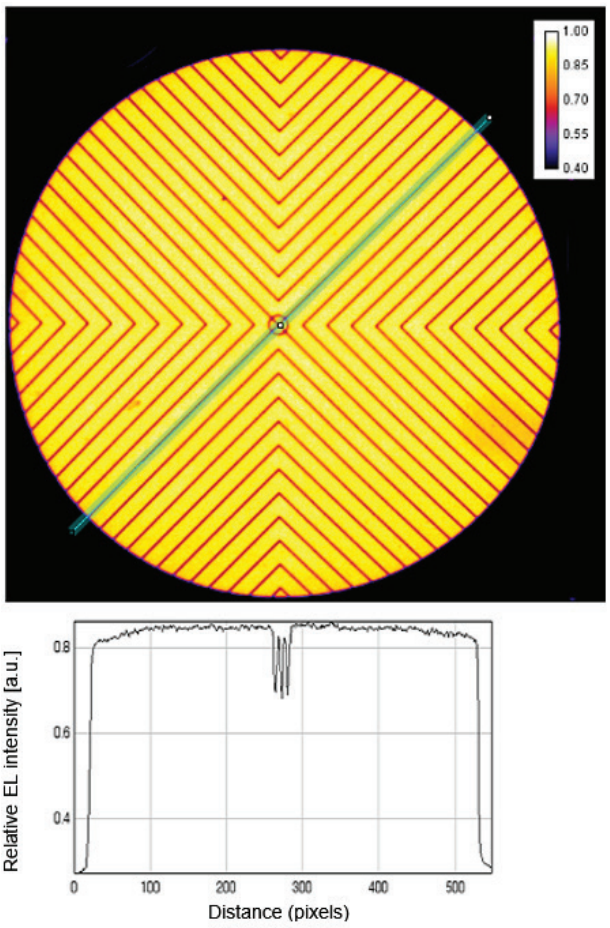

Figure 2: Top: Normalized EL image of a SJ-SS GaAs LPC at an injection current of 1 mA. The metallized front grid is visible as dark lines in the EL image. Bottom: Plot of the normalized EL along line scan, marked with cyan, showing an even distribution of the current. Note that the line used for the line scan is actually a rectangle, which covers a narrow area of the LPC beside the central finger.

only placed in the top right and bottom right corner (compare Fig. 1b), of which only the three wire bonds in the top right corner were electrically contacted during the measurements described in this work. Thus, the injected current needs to redistribute from the top right corner to the rest of the busbar metallization. For high current conditions the narrowest sections of the busbar represent a significant bottleneck to the current flow, resulting in a significant voltage drop at those points. For a device contacted in all four corners, this voltage drop would not occur and the EL profile is expected to be radially symmetrical, with the EL signal decaying from the border to the center of the active area. A second effect is seen as a decay of EL from the top right corner to the center of the LPC. This effect can be explained by a voltage drop at the grid and top surface resistance and would stay the same, regardless the connection of the LPC to the external contacts. A combination of both effects, can be clearly seen in normalized EL along the line scan, marked with a cyan line in Figure 3. To mitigate resistance losses from lateral conduction above the pn-junction, recent designs of LPCs employ a so-called lateral conduction layer [17]. This layer is composed of a highly doped material with a bandgap larger than the photon energy of the impinging light – making it transparent for the used laser wavelength.

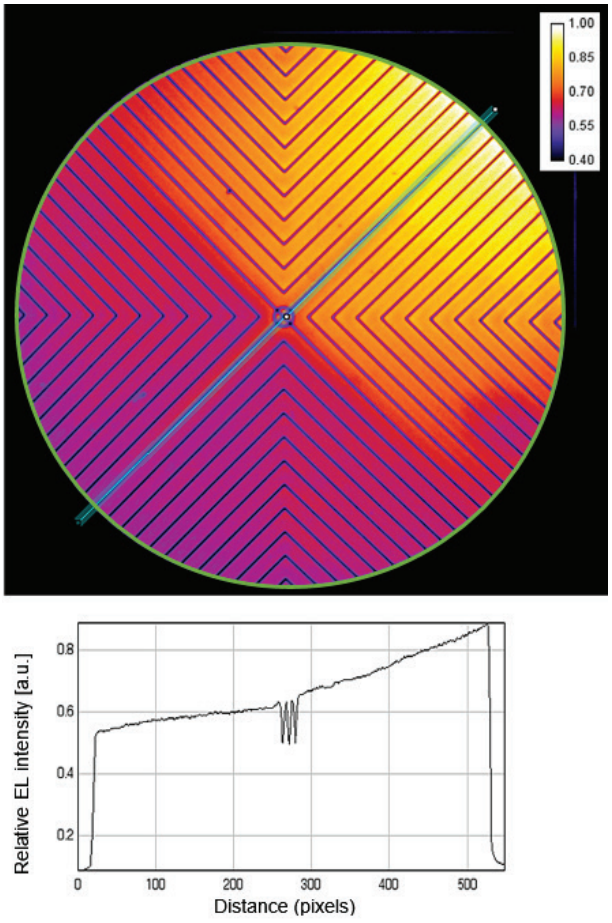

Figure 3: Top: Normalized EL image of a SJ-SS GaAs LPC with injection current 400 mA. The metallized front grid is visible as dark lines in the EL image. Bottom: Plot of normalized EL along a line scan, marked with cyan, showing a combination of various resistances on the EL profile through the active area. Note that the line used for the line scan is actually a rectangle, which covers an area of the LPC beside the central finger. The green circle marks the central active region, taken for calculations of the relative quantitative analysis.

In addition to the qualitative assessment of the current distribution, the spatially resolved EL measurements can also be assessed for a relative quantitative analysis. Therefore, the mean pixel value of the circular active region (marked with a green circle in Figure 3) is calculated and used for normalization of all EL images (various injection currents and temperatures). In Figure 4 the resulting counts per second are plotted, as recorded by the CCD camera after subtraction of the dark image. Consequently, this value corresponds to the dependency of the EL intensity on the injection current and temperature.

The shapes of the EL curves can be described by a power-law current dependence [18].

$$EL_{\frac{counts}{s}}(T) = k_{CCD}\, C(T)\, I^{b(T)} \tag{1}$$

k_{CCD} is the efficiency of CCD sensor and optics and $C(T)$ and $b(T)$ are in general temperature dependent coefficients. Similar behavior of EL vs. current was previously observed for various photovoltaic devices [16], [19, 20].

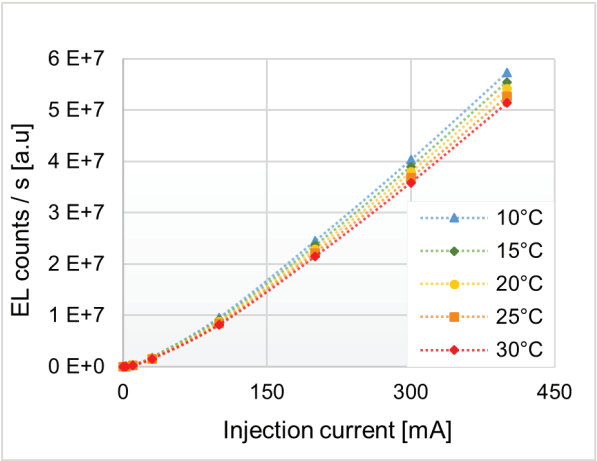

Figure 4: Plot of EL intensity vs. injection current from SJ-SS GaAs LPC extracted from mean pixel values of processed EL images at various temperatures.

In Figure 6 the EL intensity is plotted normalized to the value at T=10°C as a function of temperature. As can be seen, for all injection currents the EL intensity decreases with increasing temperature. The corresponding negative temperature coefficient depends on injection currents. Increasing temperature has a larger impact on EL for lower injection currents as seen in Figure 5. Temperature coefficients dEL/dT change from -1.5 %/°C for injection current of 1 mA to -0.5 %/°C for injection current of 400 mA.

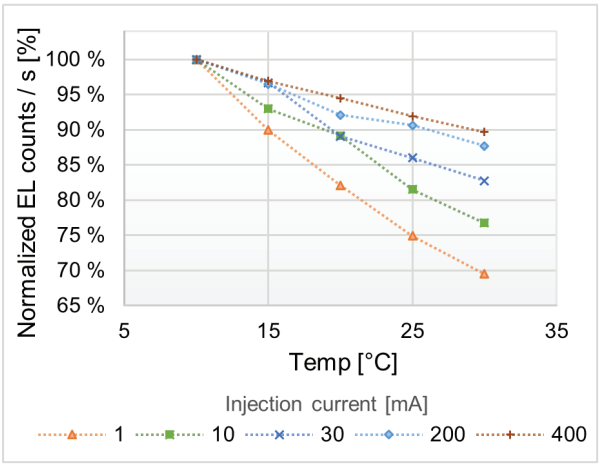

Figure 5: Temperature dependence of the EL intensity extracted from mean pixel values of processed EL images at different injection currents.

5.2 Spectrally resolved measurements

While spatially resolved EL characterization enables quick, qualitative analysis, it lacks information on the spectral distribution of the emitted light. Since the spectrum of emitted light corresponds to the bandgap of the direct semiconductor, it provides information about the change of the absorber material's bandgap with temperature. As can be seen in Figure 6, increasing temperature results in two different effects: Firstly, the EL emission peak is shifted to lower energies, as expected due to the dilation of the crystal lattice and corresponding decrease in bandgap described by the following equation [21]:

$$E_g = E_0 - \alpha \frac{T^2}{T + \beta} \qquad (2)$$

where E_g is the bandgap and E_0, α and β are material dependent parameters. The measured temperature coefficient dE_{g_meas}/dT = -0.46 meV/K agrees well with the published value for that temperature range dE_{g-pub}/dT = 0.45 meV/K [22, 23].

Secondly, it provides insight into how EL emission decreases with rising temperature. While the slope at lower energies (i.e. below the bandgap) remains constant, the slope at higher energies (i.e. above the bandgap) decreases with increasing temperature. This has been observed and explained before [4].

In a PoF system, the LPC is illuminated by a laser diode. Since the laser diode will typically be temperature controlled, the wavelength and thus photon energy of the laser will be constant. With maximal absorption current generation results of the impinged monochromatic light is maximized.

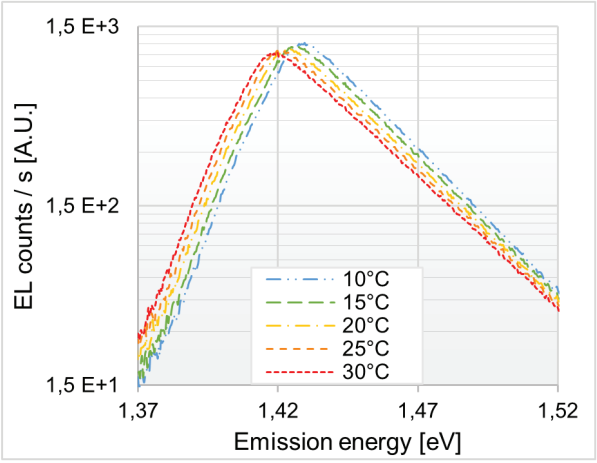

Figure 6: Spectral EL emission of SJ-SS GaAs LPC under constant injection current of 400 mA for various temperatures.

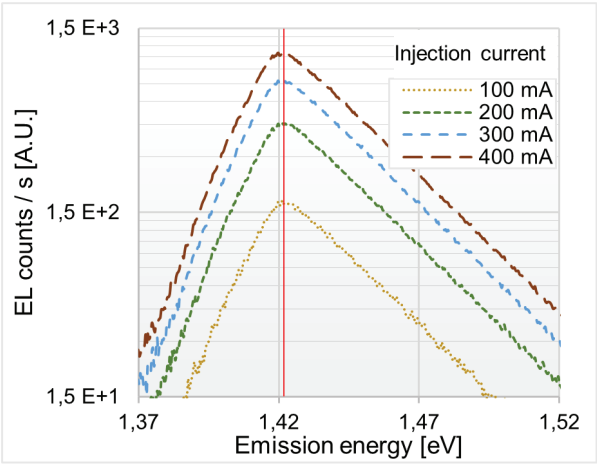

Figure 7: Spectral EL emission of a SJ-SS GaAs LPC at constant temperature of 25 °C at various injection currents. The red line marks the emission peak at 1.422eV (≈872 nm).

To ensure maximal absorption the the photon energy has to be slightly smaller than the bandgap of the LPC absorber material [7]. However, the difference should be small, as the difference in photon and bandgap energy represents an energy loss. It is mainly converted

into heat due to thermalisation of the photo excited carrier towards the band edge. Consequently, a temperature induced drop of E_g leads to increased thermalisation losses for constant photon energy. In other words, since the energy needed to generate an electron-hole pair will decrease with increasing temperature, all excess energy carried by photons of constant wavelength will result in thermal losses. This in turn increases the device temperature even further until an equilibrium is reached.

Injection current dependent spectra at constant temperature are plotted in Figure 7. For the investigated range it can be seen, that the shape of the emission spectra is independent of the injected current.

6 Conclusions

A spatial EL analysis of a SJ-SS LPC sample provided insight on the current distribution and resistive losses of the device under test. It was shown that the magnitude of the EL signal depends on temperature. Thus, for quantitative analysis it is important to take the dependence on temperature into account.

Spatial EL under forward injection current of 1 mA showed that the material and manufacturing quality is homogeneous across the device. Under injection current of 400 mA, a drop in the EL signal from the top right to the lower left side was observed, which can be explained with non-ideal electrical contacting of the device. For optimal performance of the investigated sample, electrical contacts for both EL measurements and operation should be established equally in all four corners.

Temperature dependent spectral EL measurements gave insight into the change of bandgap with increasing temperature. For a Power-over-Fiber system, where the laser diode is typically actively cooled and, thus, the wavelength (=photon energy) stays constant, a temperature induced decrease of absorber bandgap leads to increased thermalisation losses, since photo generated carriers will lose the excess energy by interacting with the crystal lattice and thermalize down to the band edge.

7 Acknowledgments

The authors thank M. Bokalič for fruitful discussions about EL and measurement support and Kasimir Reichmuth for proofreading and comments on the manuscript. The authors acknowledge the financial support from the Slovenian Research Agency (program P2-0197 and PhD funding for R.K.).

8 References

1. A. Delamarre, L. Lombez, and J.-F. Guillemoles, "Characterization of solar cells using electroluminescence and photoluminescence hyperspectral images," *J. Photonics Energy*, vol. 2, no. 1, pp. 027004–1, 2012.
2. J. A. Giesecke, M. Kasemann, and W. Warta, "Determination of local minority carrier diffusion lengths in crystalline silicon from luminescence images," *J. Appl. Phys.*, vol. 106, no. 1, p. 014907, Jul. 2009.
3. U. Rau, "Reciprocity relation between photovoltaic quantum efficiency and electroluminescent emission of solar cells," *Phys. Rev. B*, vol. 76, no. 8, p. 085303, Aug. 2007.
4. C. Karcher, H. Helmers, M. Schachtner, F. Dimroth, and A. W. Bett, "Temperature-dependent electroluminescence and voltages of multi-junction solar cells," *Prog. Photovolt. Res. Appl.*, vol. 22, no. 7, pp. 757–763, Jul. 2014.
5. J.-G. Werthen, S. Widjaja, T.-C. Wu, and J. Liu, "Power over fiber: a review of replacing copper by fiber in critical applications," 2005, p. 58710C–58710C–6.
6. V. Sittakul, L. R. Clare, S. G. Burrow, X. C. Li, and M. J. Cryan, "Power-over-fibre for wireless applications," *Microw. Opt. Technol. Lett.*, vol. 53, no. 5, pp. 1027–1032, May 2011.
7. O. Höhn, A. W. Walker, A. W. Bett, and H. Helmers, "Optimal laser wavelength for efficient laser power converter operation over temperature," *Appl. Phys. Lett.*, vol. 108, no. 24, p. 241104, Jun. 2016.
8. J. Schubert, E. Oliva, F. Dimroth, W. Guter, R. Loeckenhoff, and A. W. Bett, "High-Voltage GaAs Photovoltaic Laser Power Converters," *IEEE Trans. Electron Devices*, vol. 56, no. 2, pp. 170–175, Feb. 2009.
9. R. Kimovec and M. Topič, "Comparison of Measured Performance and Theoretical Limits of GaAs Laser Power Converters under Monochromatic Light", Electronics and Energetics Vol. 30, No 1, DOI: 10.2298/FUEE1701093K, pp. 93 – 106, 2017.
10. K. Worms, C. Klamouris, F. Wegh et al, "Reliable and lightning-safe monitoring of wind turbine rotor blades using optically powered sensors," *Wind Energy*, 2016, DOI: 10.1002/we.2009
11. Y. Tanaka, T. Shioda, T. Kurokawa, J. Oka, K. Ueta, and T. Fukuoka, "Power line monitoring system using fiber optic power supply," *Opt. Rev.*, vol. 16, no. 3, pp. 257–261, 2009.
12. J. Turan, L. Ovsenik, and J. Turan Jr, "Optically Powered Fiber Optic Sensors," *Acta Electrotech. Inform. No*, vol. 5, no. 1, p. 3, 2005.
13. G. Bottger, M. Dreschmann, C. Klamouris, M. Hubner, M. Roger, A. W. Bett, T. Kueng, J. Becker, W. Freude, and J. Leuthold, "An Optically Powered

Video Camera Link," *IEEE Photonics Technol. Lett.*, vol. 20, no. 1, pp. 39–41, Jan. 2008.
14. R. Peña and C. Algora, "One-watt fiber-based power-by-light system for satellite applications," *Prog. Photovolt. Res. Appl.*, vol. 20, no. 1, pp. 117–123, Jan. 2012.
15. J. G. Werthen, M. J. Cohen, T. C. Wu, and S. Widjaja, "Electrically isolated power delivery for MRI applications," in *Proc. Int. Soc. Magn. Reson. Med. Annu. Meeting, Seattle, WA*, 2006, p. 1353.
16. M. Bokalič, J. Raguse, J. R. Sites, and M. Topič, "Analysis of electroluminescence images in small-area circular CdTe solar cells," *J. Appl. Phys.*, vol. 114, no. 12, p. 123102, Sep. 2013.
17. E. Oliva, F. Dimroth, and A. W. Bett, "GaAs converters for high power densities of laser illumination," *Prog. Photovolt. Res. Appl.*, vol. 16, no. 4, pp. 289–295, Jun. 2008.
18. K. Wang, D. Han, and M. Silver, "The Power Law Dependence of Electroluminescence Intensity on Forward Current in a-Si:H p-i-n Devices," in *Symposium A – Amorphous Silicon Technology - 1994*, 1994, vol. 336, p. 861 (6 pages).
19. K. J. Price, A. Vasko, L. Gorrelland, and A. D. Compaan, "Temperature-Dependent Electroluminescence from CdTe/CdS Solar Cells," in *Symposium B – Compound Semiconductor Photovoltaics*, 2003, vol. 763, p. B5.9 (6 pages).
20. M. Seeland, R. Rösch, and H. Hoppe, "Quantitative analysis of electroluminescence images from polymer solar cells," *J. Appl. Phys.*, vol. 111, no. 2, p. 024505, Jan. 2012.
21. Y. P. Varshni, "Temperature dependence of the energy gap in semiconductors," *Physica*, vol. 34, no. 1, pp. 149–154, Jan. 1967.
22. C. D. Thurmond, "The Standard Thermodynamic Functions for the Formation of Electrons and Holes in Ge, Si, GaAs , and GaP," *J. Electrochem. Soc.*, vol. 122, no. 8, pp. 1133–1141, Aug. 1975.
23. P. Lautenschlager, M. Garriga, S. Logothetidis, and M. Cardona, "Interband critical points of GaAs and their temperature dependence," *Phys. Rev. B*, vol. 35, no. 17, pp. 9174–9189, Jun. 1987.

Arrived: 31. 08. 2016
Accepted: 22. 09. 2016